Reduced Order Model of a Human Left and Right Ventricle Based on POD Method

Piotr Przybyła, Witold Stankiewicz, Marek Morzyński, Michał Nowak, Dominik Gaweł, Sebastian Stefaniak, and Marek Jemielity

1 Introduction

According to the World Health Organization, chronic diseases are responsible for 63% of all deaths in the world, with cardiovascular disease as the leading cause of death. Magnetic resonance imaging technologies have advanced rapidly in recent years enabling both radiologists and cardiologists to perform evaluated studies for assessment of the functional parameters of the heart, such as myocardial wall motion, volumetric parameters, ejection fraction, and stroke volume across both the left and right ventricles. In theory the term cardiomyopathy could apply to almost any disease affecting the heart, in practice it is usually reserved for severe myocardial disease leading to heart failure [1]. Clinical biomechanists are confronted with various challenges. One of them is the task of reducing the amount of data from clinical datasets [2, 3].

Recently computer methods and programs are being implemented throughout all aspects of biomedical research and medical practice. Many of them are concentrated on biomechanics of particular movement disorders, as in the case of hip joint dysplasia [4], Parkinson disease [5], or cardiac motion [6]. In the last case, to mark the deteriorations, clinical biomechanists record kinematic and electromyographic signals, which are both analyzed statistically and in terms of an explicit inverse dynamic model [7]. These analyses, on the other hand, may grant insight into proper relevant biomechanical aspects of particular movement disorders and, in some cases, elemental motor deteriorations. Nevertheless, magnetic resonance imaging brings

P. Przybyła • W. Stankiewicz (✉) • M. Morzyński • M. Nowak • D. Gaweł
Division of Virtual Engineering, Poznan University of Technology, Poznań, Poland
e-mail: witold.stankiewicz@put.poznan.pl

S. Stefaniak • M. Jemielity
Cardio-Surgery Department in Clinical Hospital of University of Medical Sciences Poznan, Poznań, Poland

A. Wittek et al. (eds.), *Computational Biomechanics for Medicine*,
DOI 10.1007/978-3-319-54481-6_5

a large amount of data which is difficult to elaborate and process. The design of the model of heart motion is difficult as the movement interweaves with several factors such as muscle contraction, blood flow, calcification, fiber orientation, and nerve impulses. Each of those aspects can be designed separately and is challenging as well. The example of computational model combining all the aforementioned factors is given in [8].

Another solution can be a "Black Box" model based on statistical analysis. An overview of these methods, combining different types of models over a global shape model and promising for other medical segmentation problems, especially if local anatomical abnormalities (e.g., a tumor) appear, is presented in [9].

In [10] clinical diagnosis is based upon global modes of motion, measurement of longitudinal displacement of the LV may be critical, and thus an increased emphasis on acquiring sufficient long axis image data may be warranted. They also suggest that methods sensitive to transmural differences in displacement may offer a clinical advantage for diagnosis of functional abnormality. Finally, the creation of a kinematic mode database can greatly increase reconstruction efficiency in healthy hearts by eliminating modes which contribute little to the reconstruction accuracy [11].

We can create a "black box model" based only on movement observation, which could be applied in, for example, flow control. Mathematical models for human ventricles contain large amounts of data. Their numerical solution is based on appropriate space/time discretizations which requires computational times that even utilizing state-of-the-art algorithmic solvers are far from being acceptable. A means to overcome this difficulty is to use reduced order models (ROMs) where the dimension of the ROM is, by at least one order of magnitude, smaller than the dimension of the full order model while still separating the effects of the essential dynamics of the underlying physiological processes. Suitable model order reduction techniques include balanced truncation (BT) [12], Proper Orthogonal Decomposition (POD) [13], and reduced basis methods (RBM) [14].

This paper is structured as follows. In Sect. 2 we describe the method of generating a model of left and right ventricle. In Sect. 3 we present Proper Orthogonal Decomposition. Decomposition of left and right ventricle and decomposition of left ventricles are presented in Sects. 4 and 5, respectively. Finally, discussion and conclusions are presented in Sect. 6.

2 Generation of a Patient-Specific Cardiac Model

Choosing an optimal medical image visualization method always raises many questions. With a choice between CT, ultrasonography, Spectral CT, and MRI, the Magnetic Resonance Imaging seems to be the most suitable—while CT slices are more dense, they are related with radiation.

Initial clinical data consists of a cine-MRI sequence of the cardiac cycle of an adult patient. Images are in short axis, covering both ventricles (ten slices; slice

thickness: 8 mm, temporal resolution: 25 frames). Images were made isotropic and contrast was enhanced by clamping the tails of the grey-level histogram. DICOM examinations were loaded into the program, in particular, dynamic information on a cardiac study is automatically extracted.

To build a patient-specific model of the heart from the DICOM data resulting from MRI, it is crucial to segment the different parts of the organ. That implies segmenting the left and right endocardia, as well as the epicardium.

In this paper, we demonstrate our methodology on commonly available datasets. They consist of left and right ventricle data by Toussaint et al. [7], and a set of left ventricle models from the Sunnybrook Cardiac Data, SCD [15]. In the first case, interactive surface generation using implicit functions was used. Segmentation is started on the first frame of the MRI cardiac sequence, corresponding to end diastole. Interactive segmentation is based on variational implicit surfaces [16], which consists of computing an implicit function whose zero-level set passes through defined control points (landmarks). In order to calibrate the physiological parameters of the model, segmentation operation is repeated throughout the entire cardiac sequence, in order to estimate—for instance—the blood pool volume. The semi-automatic process described above, in which the user empirically specifies landmarks and filters, is to ensure the visual compliance of the myocardium area in the MRI and the determined mask. Then, nonlinear image registration based on diffeomorphic demons is performed [17]. The resulting deformation fields are then used to propagate the myocardium mask throughout further frames of cardiac sequence. Finally, the dynamic mesh of the myocardium is obtained by performing successive isosurface extractions on the aforementioned binary masks.

3 Proper Orthogonal Decomposition

Modal decomposition is a powerful and popular tool in model reduction techniques [18] and biomechanics [13]. In the case of the empirical approach, where the modes are obtained from the analysis of measured data or simulation, a number of methods may be distinguished. The most popular of them, Proper Orthogonal Decomposition (POD) (also known as PCA—Principal Component Analysis) [19–21] is based on the eigenanalysis of the autocorrelation matrix computed for the input signal [22]. There are many variants of this method designed for certain purposes. For example, method of snapshots [23] is used when the number of snapshots is much smaller than the dimension of the single snapshot. Sparse PCA [24] finds modes that are sparse vectors, that facilitates further interpretation. Kernel PCA [25] is the extension of PCA using kernel functions for the mapping of input data onto higher-dimensional feature space and multilinear PCA [26] is based on the linear transformations of each dimensional separately.

Another decomposition methods used in biomechanics include Independent Component Analysis [27] and Linear Discriminant Analysis (LDA) [28].

In the case of global analysis of cyclic data, snapshot POD of Sirovich is the best approach. This method is based on the assumption that there is a correlation between sampled data and it decomposes the data into uncorrelated modes that are optimal for energy representation by construction.

In this method, the M snapshots v_i of size N (number of Degrees of Freedom) are centered using time-averaged solution u_0. Resulting M fluctuation vectors $v_i' = v_i - u_0$ form a matrix V'. POD modes used in model reduction are the eigenvectors u_i of standard eigenproblem $Cu_i = \lambda_i \cdot u_i$ of the autocorrelation matrix C. In snapshot POD, this matrix (of size $M \times M$) is defined as:

$$C = \frac{1}{M} V'^T V',$$

and the POD modes w_i are computed by the projection of eigenvectors u_i, related to eigenvalues λ_i of largest magnitude and representing mode amplitudes, onto a set of initial snapshots V:

$$w_i = \frac{Vu_i}{\|Vu_i\|}.$$

4 Proper Orthogonal Decomposition of Left and Right Ventricle

A set of meshes was created with the help of CardioViz [29, 30], containing the 85 frames of the cardiac cycle. Vertex positions at each time frame are assigned to the corresponding frame mesh. As the topology of the mesh does not change along the sequence, a single VTK object explaining the topology is given to all the frames. Scalar data are also associated with each time frame. Linear interpolation is used to map scalar information on the mesh object [7]. Proper orthogonal decomposition was implemented to one cardiac cycle. The cycle was decomposed to 85 modes, which should represent 100% energy of heart motion. The Table 1 presents individual and joint information transferred by modes. We note the first five modes only, by virtue of little percentage of information being transferred by further modes, assuming that they can be neglected. It can be seen that just the first three modes represent 99% of information concerning the cardiac cycle. Using this data we can judge, which modes seem to be the important.

The first three modes, multiplied by maximal and minimal values of coefficients and superimposed on the time-average geometry of the heart, are presented in Fig. 1. In order to strengthen the visual effect, the results are scaled twice. The first mode represents systole of both left and right ventricles, with no twist.

The twist and movement along long axis are described by the second and third POD modes (Figs. 2 and 3, respectively).

Table 1 Information transferred by modes

Mode number	Information transferred [%]	Information transferred (jointly) [%]
1	73.55	73.55
2	22.14	95.70
3	3.43	99.13
4	0.49	99.63
5	0.14	99.77

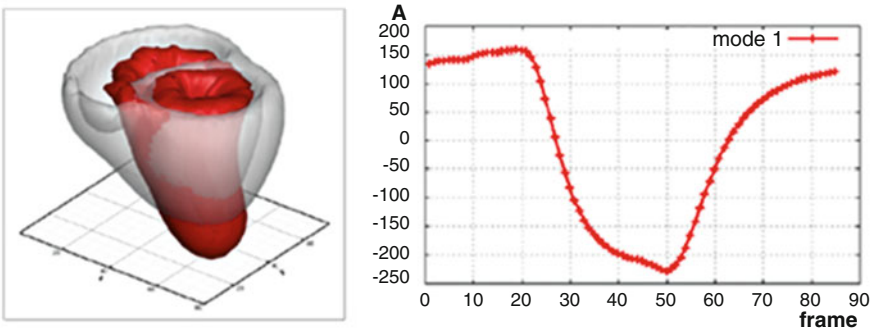

Fig. 1 The First POD mode superimposed on averaged geometry, depicted using doubled min. and max. values of corresponding time coefficient (dimensionless mode amplitude A)

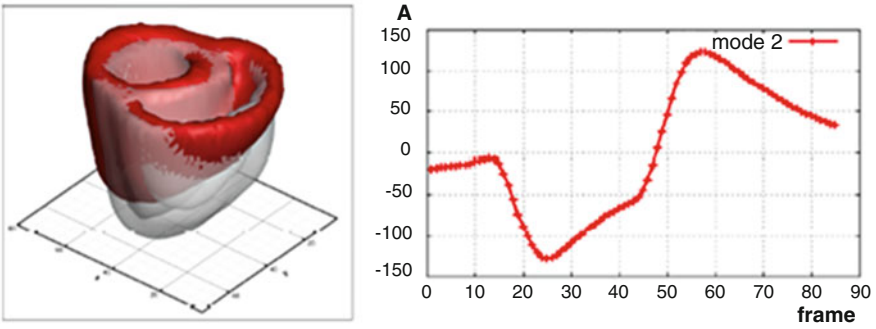

Fig. 2 Same as Fig. 1, but for the second POD mode

The figures above display slight discrepancy in amplitude at the beginning and end of the cycle. We assume that the reason for this is the absence of snapshots for one or two time steps. Diagrams of specific modes are distinctive to a factual, individual heart model [7], in this case left and right ventricle with no pathologies. Pathological ventricles will have differing, individual diagrams.

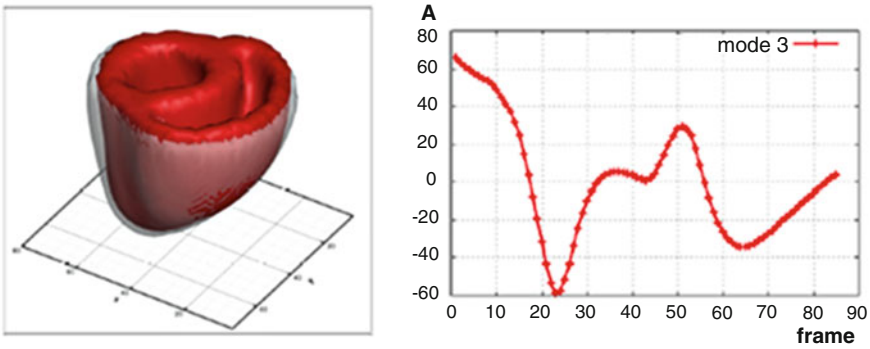

Fig. 3 Same as Fig. 1, but for the third POD mode

5 Proper Orthogonal Decomposition of Left Ventricles

Proper Orthogonal Decomposition was performed on models from The Sunnybrook Cardiac Data (SCD) [15], also known as the 2009 Cardiac MR Left Ventricle Segmentation Challenge data, consisting of models from a mixed groups of patients and pathologies. The data contributor is the Imaging Research, Sunnybrook Health Sciences Centre, Toronto, Canada. The subset of the data was first used for automated myocardium segmentation challenge from short-axis MRI, held by a MICCAI workshop in 2009. The data has already been registered [15]. The study description indicates the pathology. The patient datasets were classified into four groups representing diverse morphologies, based on the following clinical criteria [31]:

I. Heart failure with infarction (SC-HF-I) group had EF < 40% and evidence of late gadolinium (Gd) enhancement (12 patients)
II. Heart failure with no infarction (SC-HF-NI) group had EF < 40% and no late Gd enhancement (12 patients)
III. LV hypertrophy (SC-HYP) group (EF > 55%, 12 patients)
IV. Healthy (SC-N) group had EF > 55% and no hypertrophy (nine patients).

Three groups of patients (I, II, and IV) were chosen for further analysis of modal decomposition. The results were presented for the most exemplary of them.

5.1 Ventricle Models with Heart Failure with Infarction

Modal distribution of the same pathology seems to be comparable between different patients. Proportional information of mode I does not exceed 60%. As proportional information we understand the shared information of movement carried by mode. The same phenomena applies to mode II and III. Mode II holds on the level between

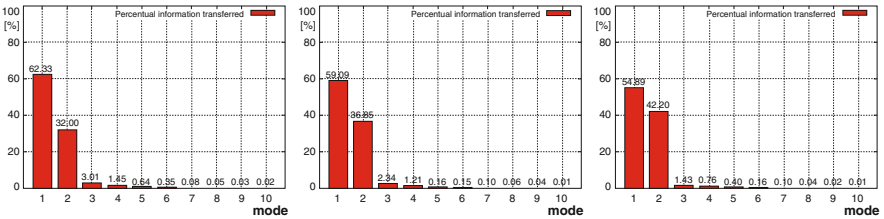

Fig. 4 Proportional information transferred by the modes. Three different patients with heart failure with infarction presented from left to right

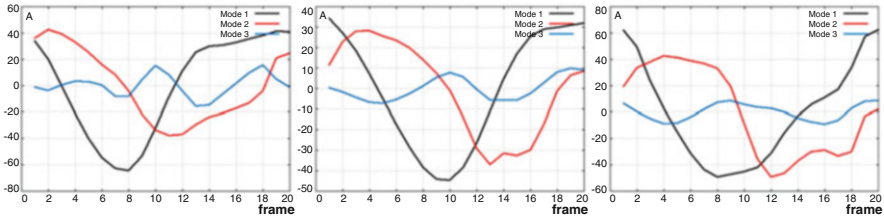

Fig. 5 Mode amplitudes A in time, for three different patients with heart failure with infarction

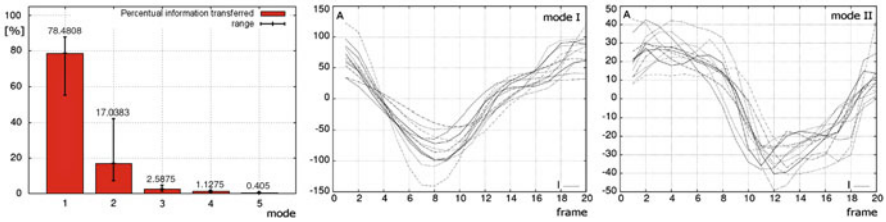

Fig. 6 Amplitude range overview through modal distributions of mode I, II, III for all test cases. Mode amplitudes A in time (frames of cycle), presented for every test case, mode I and mode II

30% and 42%, while mode III does not exceed 3%. Proportional distribution for three exemplary patients: men aged 48, 57, 69 is shown in Fig. 4.

Changes of amplitudes in time for the first three modes in Fig. 5 for exemplary patients are congenial. Transition of graphs appears almost simultaneously (mode I and III) showing little differences between mode II (patient II and III has similar progress; the curve of patient I is flattened at the beginning of the cycle).

Figure 6 displays the amplitudes of mode I and II in time for every test case of the presented group. Thorough analysis will require full medical history of every single patient, which was not provided in the data. However it is noticeable, that changes of amplitude are congenial.

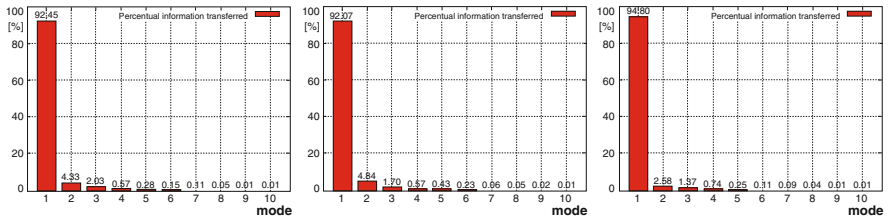

Fig. 7 Proportional information transferred by the modes. Three different patients with healthy hearts presented from left to right

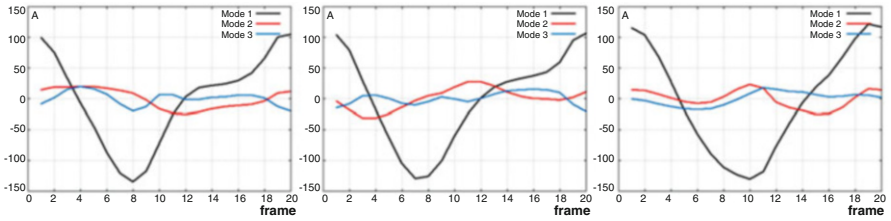

Fig. 8 Mode amplitudes A in time, presented for three different patients with healthy hearts

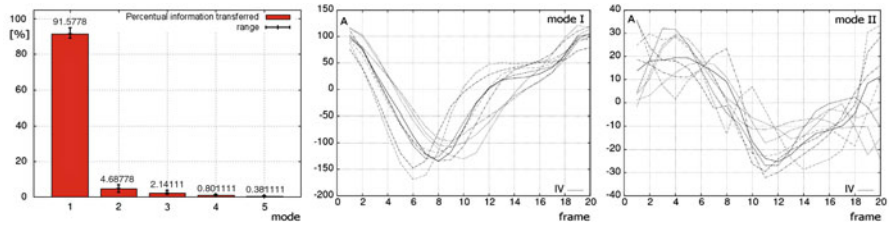

Fig. 9 Amplitude range overview through modal distributions of mode I, II, III for all test cases. Mode amplitudes A in time (frames of cycle), presented for every test case, mode I and mode II

5.2 Healthy (SC-N) Group, no Hypertrophy

Exemplary distributions of healthy patients: 63 aged male, 53 aged female, 77 aged female, is presented in Fig. 7. In this case, mode I substantially dominates in proportional information distribution. There is little influence of modes II and III. Similar phenomena appeared in the model of left and right ventricle in Sect. 4.

Range of amplitude in time for first three modes in Fig. 8 for healthy patients is almost identical, even though we compare patients from differing ages and gender. The averaged value of mode I from acquired dataset is 91.35%.

In Fig. 9 we have presented the amplitudes of mode I and II in time for every test case of the presented group. The shape of amplitudes is similar, and the tendency is maintained for every test case in both modes.

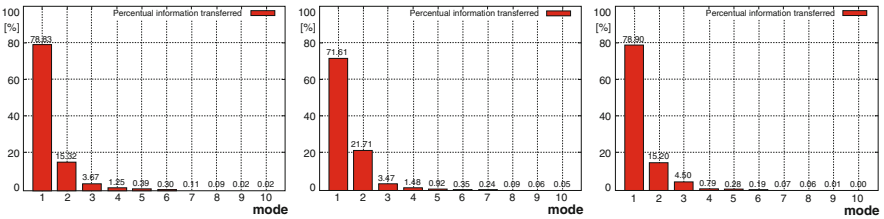

Fig. 10 Proportional information transferred by the modes. Three different patients with heart failure without infarction presented from left to right

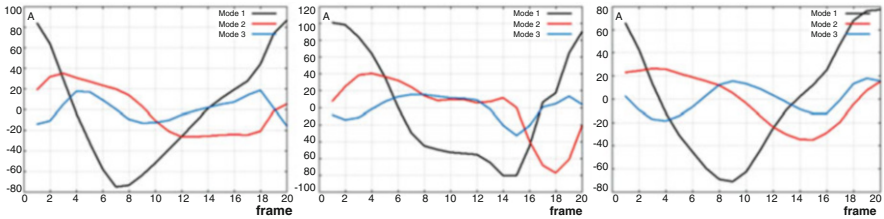

Fig. 11 Mode amplitudes A in time, presented for three different patients; heart without infarct

5.3 Heart Failure with no Infarction

The third group of patients analyzed in this paper were having heart failure without infarct. In these cases, achieved data indicates greater influence for mode II in pathological hearts than for healthy ones. However, it was still less than for patients with heart failure with infarct. Three exemplary test cases (77 aged male, 82 aged male, 77 aged female) are presented in Figs. 10 and 11.

Mode amplitude is fluctuating in mode II and III, while mode I is similar in all presented cases. Average value of mode I for patients with no infarction fluctuates between 70% and 80%, while mode II exceeds 15%, which is rather unique, and characteristic for this pathology.

In Fig. 12 we have presented the amplitudes of mode I and II in time for every test case of the presented group. It is notable, that amplitudes are similar to these presented in Sect. 5.1. As mentioned before, thorough analysis could be performed with closer information about patients pathology. However, general trend of amplitudes is maintained.

6 Discussion and Conclusions

This article concerns the analysis of the motion of the left and right ventricle, captured from MRI examination. We have proven that such a complex motion might be modeled with a few degrees of freedom—POD modes and their amplitudes.

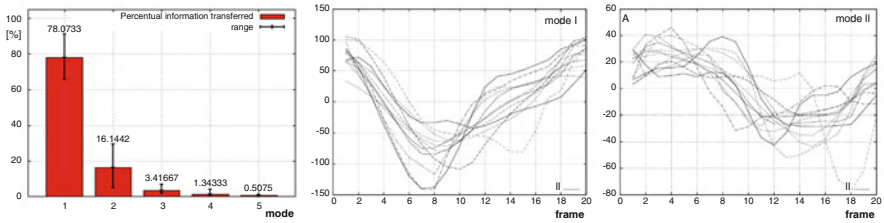

Fig. 12 Amplitude range overview through modal distributions of modes for all test cases. Mode amplitudes A in time (frames of cycle), presented for every test case, mode I and mode II

Modal decomposition gives more insight into the heart than 2D analysis of MRI slices. This approach is in line with the recent works. Principal Component Analysis has been already used to analyze the electrocardiogram signals for detection of heart arrhythmia [32], reduced order modeling [33], and automated diagnosis of cardiac health [34]. Recently, 4D models are used as an input. Wu et al. [35] use POD to analyze time-varying, three-dimensional data from ECG-gated multislice cardiac CT images of human right ventricle and classify pulmonary hypertension. They state that such approach might provide "new metrics to improve the diagnosis and understanding of cardiovascular diseases." Similar approach for cardiac MR and CT image sequences is used by Perperidis et al. [29].

In our study, already three modes allow to reproduce 99% of the original properties of the heart motion, to analyze it and compare to the real motion of systole and diastole. It will make possible the correlation of modal data (modes, amplitudes, and eigenvalues) with the corresponding pathologies. As the change in the cardiac cycle will be visible after the spatio-temporal decomposition as well, the designed model makes the proper diagnosis, preparation for invasive procedures and future treatment much easier, more cost effective and requiring less time.

The analyzed set is quite small, but preliminary conclusions may be drawn. It seems that the increased eigenvalue of second mode (related to higher amplitudes) might be correlated with the aforementioned heart failures. The order of the higher modes might vary for different subjects. The first modes always represent the contraction of the ventricles. The differentiation between failing and healthy hearts is done by comparing ratios of the first mode (failing below 89–91%) and second mode (failing above 5.1–6.7%), no matter what motion it describes. Unfortunately, myocardial infarction does not affect noticeably the modal amplitudes and eigenvalues. This case requires further study, performed on a larger patients group.

The POD analysis can show abnormalities which cannot be observed in live time diagnostics, before any dysfunction or symptoms arise. This would allow the prevention of changes in cardiac muscle by early diagnosis and treatment either pharmacologically or surgically. A major significance of this work is that we would be able to diagnose various hearts, including the prenatal heart. MRI examination is both suitable and safe for in utero scans of the fetal heart. As an example, let us consider the left ventricle ejection fraction. The normal value is more than 50%,

when it falls below, it is identified as left ventricle dysfunction. As we know from its movement we are able to "switch off or disregard" this specific part of the muscle and we will not receive any important information about the disease, because the LVEF will remain >50%. This could present in heart infarct, cardiomyopathy, dangerous heart infections, and other states. The use of POD can show that despite the normal ejection fraction, another underlying disease may be present. The cardiac movement preceding the heart conduction system has been known to have been misdiagnosed. The conductive system leads the impulse to start the systole from the apex to the bases. Conduction problems with the impulse may not been seen as a delay of diastole or systole within the muscle segment. The large more obvious issues are easily appreciated, however, the smaller more subtle issues are not easily perceived and unfortunately they often go unnoticed. The POD method is ideally suited for quick diagnosis of these types of abnormalities. Last but not least this is an excellent tool for the presentation and teaching of cardiac abnormalities, for both medical students and as a tool for Cardiac specialists.

An important limitation of the method is the need of registration of the data resulting from medical imaging. While there are software tools for such handling available, they still do not allow full automation. The quality of the data, like the resolution of MRI slices, is related to the above—it might influence the order of (further) modes, their shapes, and eigenvalues.

Acknowledgments This work was supported by The National Centre for Research and Development under the grant PBS3/B9/34/2015.

References

1. Baguet JP, Barone-Rochette G, Tamisier R, Levy P, Pépin JL (2012) Mechanisms of cardiac dysfunction in obstructive sleep apnea. Nat Rev Cardiol 9(12):679–688
2. Bouvy ML, Heerdink ER, Leufkens HGM, Hoes AW (2003) Predicting mortality in patients with heart failure: a pragmatic approach. Heart 89(6):605–609
3. Bassingthwaighte J, Hunter P, Noble D (2009) The cardiac Physiome: perspectives for the future. Exp Physiol 94(5):597–605
4. Rychlik M, Józwiak M, Idzior M, Chen PJ, Szulc A, Woźniak W (2010) Acetabular direction and capacity of hip joint dysplasia in cerebral palsy–counterpoint option of morphology understanding. In 6th World Congress of Biomechanics (pp. 1546–1549), Springer
5. Fasano A, Daniele A, Albanese A (2012) Treatment of motor and non-motor features of Parkinson's disease with deep brain stimulation. Lancet Neurol 11(5):429–442
6. Glass L, Hunter P, McCulloch A (eds) (2012) Theory of heart: biomechanics, biophysics, and nonlinear dynamics of cardiac function. Springer, New York
7. Toussaint N, Mansi T, Delingette H, Ayache N, Sermesant M (2008) An integrated platform for dynamic cardiac simulation and image processing: application to personalised tetralogy of fallot simulation. In: Eurographics Workshop on Visual Computing and Biomedicine. (pp.21–28).
8. Vazquez M, Arís R, Houzeaux G, Aubry R et al (2011) A massively parallel computational electrophysiology model of the heart. Int J Num Meth Biomed Eng 27(12):1911–1929

9. Heimann T, Meinzer HP (2009) Statistical shape models for 3D medical image segmentation: a review. Med Image Anal 13(4):543–563
10. O'Dell W, McVeigh ER (1998) A modal description of LV motion during ejection, In: Proceedings of the International Society for Magnetic Resonance in Medicine
11. Hoppe RHW (2002) Model reduction by proper orthogonal decomposition, NSF-I/UCRC 288 grant, University of Houston
12. Antoulas AC (2005) Approximation of large scale dynamical systems. Advances in design and control, vol 6. SIAM, Philadelphia
13. Rychlik M, Stankiewicz W, Morzyński M (2008) Application of modal analysis for extraction of geometrical features of biological objects set. Biodevices 2008(2):227–232
14. Fischer SL, Hampton RH, Albert WJ (2014) A simple approach to guide factor retention decisions when applying principal component analysis to biomechanical data. Comput Methods Biomech Biomed Engin 17(3):199–203
15. Radau P, Lu Y, Connelly K, Paul G, Dick AJ, Wright GA (2009) Evaluation framework for algorithms segmenting short axis cardiac MRI. MIDAS J 49. http://hdl.handle.net/10380/3070
16. Turk G, O'Brien JF (1999) Variational implicit surfaces. Tech. Rep. Georgia Institute of Technology, Georgia
17. Vercauteren T, Pennec X, Perchant A, Ayache N (2007) Non-parametric diffeomorphic image registration with the demons algorithm. In International Conference on Medical Image Computing and Computer-Assisted Intervention MICCAI (pp. 319–326).
18. Toussaint N, Sermesant M, Fillard P (2007) vtkinria3d: A VTK extension for spatiotemporal data synchronization, visualization and management. In: Proceedings of Workshop on Open Source and Open Data for MICCAI.
19. Daffertshofer A, Lamoth CJ, Meijer OG, Beek PJ (2004) PCA in studying coordination and variability: a tutorial. Clin Biomech 19(4):415–428
20. Lumley JL (1967) The structure of inhomogeneous turbulent flows. Atmospheric turbulence and radio wave propagation, pp 166–178
21. Chandrashekara R et al (2003) Construction of a statistical model for cardiac motion analysis using nonrigid image registration. Inf Process Med Imaging 18:599–610
22. Zhang X, Cowan BR, Bluemke DA, Finn JP, Fonseca CG et al (2014) Atlas-based quantification of cardiac remodeling due to myocardial infarction. PLoS One 9(10):e110243
23. Sirovich L (1987) Turbulence and the dynamics of coherent structures. Parts I–III. Q Appl Math 45(3):561–590
24. Zou H, Hastie T, Tibshirani R (2006) Sparse principal component analysis. J Comput Graph Stat 15(2):265–286
25. Hoffmann H (2007) Kernel PCA for novelty detection. Pattern Recogn 40(3):863–874
26. Lu H, Plataniotis KN, Venetsanopoulos AN (2008) MPCA: multilinear principal component analysis of tensor objects. IEEE Trans Neural Netw 19(1):18–39
27. Stone JV (2005) A brief introduction to independent component analysis. In: Everitt BS, Howell DC (eds) Encyclopedia of statistics in behavioral science. Wiley, Chichester
28. Yu H, Yang J (2001) A direct LDA algorithm for high-dimensional data - with application to face recognition. Pattern Recogn 34(10):2067–2070
29. Perperids D, Mohiaddin R, Edwards P, Rueckert D (2007) Segmentation of cardiac MR and CT image sequences using model-based registration of a 4D statistical model. In: Medical Imaging (p 65121D). International Society for Optics and Photonics
30. Stankiewicz W, Roszak R, Morzyński M (2011) Genetic algorithm-based calibration of reduced order Galerkin models. Math Model Anal 16(2):233–247
31. Alfakih K, Plein S, Thiele H, Jones T et al (2003) Normal human left and right ventricular dimensions for MRI as assessed by turbo gradient echo and steady-state free precession imaging sequences. J Magn Reson Imaging 17(3):323–329
32. Ghorbanian P, Ghaffari A, Jalali A, Nataraj C (2010) Heart arrhythmia detection using continuous wavelet transform and principal component analysis with neural network classifier. Comput Cardiol 37:669–672

33. Boulakia M et al (2012) Reduced-order modeling for cardiac electrophysiology. Application to parameter identification. Int J Numer Meth Biomed Engng 28:727–744
34. Martis RJ et al (2012) Application of principal component analysis to ECG signals for automated diagnosis of cardiac health. Expert Syst Appl 39(14):11792–11800
35. Wu J, Wang Y, Simon MA, Brigham JC (2012) A new approach to kinematic feature extraction from the human right ventricle for classification of hypertension: a feasibility study. Phys Med Biol 57(23):7905–7922